Nonlinear Dynamic Analysis of Automotive Turbocharger Rotor System

S. Bala Murugan, Rabindra Kumar Behera and P. K. Parida

Abstract The present development on the automotive engines on reducing size and increasing greater fuel efficiency, and less emissions took the researchers to several challenges in turbocharger rotor system. However, the challenge towards the evolution of high-efficiency bearing systems with reliability is still over the top. The paper shows the system with dynamic analysis of nonlinear turbocharger rotor system to interpret the unstable positions during running condition. The proposed model of turbocharger in this study is examined as a uniform shaft in nature with varying lengths between two bearings which actually held between compressor end and the turbine disc. The two discs are having force unbalance and the compressor impeller exists with the seal forces. The rotor considered here is supported by bearings with the nonlinear time-varying forces as reactions at the supports. The approach in this paper is allowed to solve the transient conditions, suchlike nonlinear effects due to seal forces, time histories, and Campbell diagram. The computational models are solved with analytical equations using finite element modelling (FEM) and the obtained results are verified with ANSYS® simulations. The impacts of different operating conditions at two different speeds are studied by phase-plane diagrams to understand the stability of the system.

Keywords Dual disc rotor · Ball bearing · Seal force · FEM · Stability analysis

S. Bala Murugan (✉) · R. K. Behera
National Institute of Technology, Rourkela, Odisha 769008, India
e-mail: balamurugan8202@gmail.com

P. K. Parida
College of Engineering and Technology, Bhubaneswar, Odisha 751003, India

H. K. Voruganti et al. (eds.), *Advances in Applied Mechanical Engineering*,
Lecture Notes in Mechanical Engineering,
https://doi.org/10.1007/978-981-15-1201-8_50

1 Introduction

In much kind of machineries, nonlinear vibrations play an important phenomenon in technical applications. Most of the practical cases, the system always dominated through the nonlinear effects. The system examined here in this study, called turbocharger rotor system supported by two bearings with the nonlinear time-varying forces.

In rocket engine, generally the turbocharger is considered as a major part and it supplies the propellants with low temperature to the combustion chamber which operating at extreme high pressures. Turbochargers are regularly operated at very high speeds due to its size. The high speed of turbocharger will lead the system to a pressure drop region which below the vapour pressure causing the liquid propellant to cavitate the compressor blades. In general, the speed of the oxidizer is high due to the greater density than the fuel. The main disadvantage of this provision is making the engine further complex and less reliable.

Several researchers made their extensive contribution of analysing the turbocharger rotor-bearing system. However, past one decade, experimental and theoretical studies were carried on turbochargers and reported the analysis. Bai et al. [1] examined the consequences of nonlinear dynamic characteristics of a flexible support stiffness and system stability by using a dynamic modelling. The induced forces due to nonlinearity by seals and internal damping of rotor also included in the analysis. Son et al. [2] describe the theoretical design of a gas generator of liquid rocket engine. The produced gases by the gas generator, drives the turbopumps through turbine. An analysis based on chemical non-equilibrium and droplet vapourization was given to estimate the properties. Hu et al. [3] studied the methods for detection and health monitoring and a turbopump fault diagnosis with vector machines. Hong et al. [4] carried the test on hydraulic performance of a liquid rocket engine. Wang and Sun [5] extended the analysis of turbopump rotor with gyroscopic effects with one-dimensional finite element model. Smolik et al. [6] studied the dynamic response of the turbocharger rotor for the effects of radial clearances on bearings. Novotny et al. [7] presented an efficient and numerically stable calculation model of plain floating ring bearing.

The present study shows the dynamic stability of a rotor dynamic model of turbocharger system. The rotor system included the ball bearing with Hertzian contact forces, disc mass unbalances and forces of seal which is dynamic in nature based on the Muszynska relations. The equations which are dynamic in nature are solved using implicit scheme of Houbolt's time integration. Finally, the stability of the system with different speeds of operation is carried using frequency response and phase-plane plots.

2 Dynamic Model of Turbocharger Unit

Turbochargers are principal parts of rocket engine unit. A schematic view of turbocharger is shown in Fig. 1. The turbopump rotor is supported on two bearings and exist liquid seals at pump disc. Turbopump is considered as a simple single disc in the present task, and has an inducer and diffuser in it. The turbine produces power, and it is kept at the farthest end to drive the turbocharger system.

2.1 Dynamic Formulations of System

By using Timoshenko beam theory, a simplified rotor model of the system is considered with finite elements. The shaft elements are divided by four and five nodes thoroughly. Every node of the shaft element has the degrees of freedom (DOF) four, which includes rotational (θ_y, θ_z) and translational displacements (v, w).

For the near in-depth to the dynamic effects of the system the turbocharger parts are taken as rigid bodies which lies at two nodes 3 and 5, respectively. The nodes 2 and 4 represent the ball bearings. The hydrodynamic effect at the seals produces a force which has an extremely nonlinear in nature. The seals are placed at the discharge side of the impeller and inlet end which is equal to the element forces concerned at node 3. Moreover, the component force of mass unbalance and the forces due to gravity are considered at turbine and pump discs. Now, the kinetic and the potential energy of spinning shaft elements can be written by with the effects of bending and shearing effects as:

$$T_s = \frac{1}{2}\int_0^{\ell} \rho\left\{A(\dot{v}^2 + \dot{w}^2) + I_D(\dot{\theta}_y^2 + \dot{\theta}_z^2) + I_P\left[\Omega^2 + \Omega(\dot{\theta}_z\theta_y - \dot{\theta}_y\theta_z)\right]\right\}\mathrm{d}s \quad (1)$$

$$U_s = \frac{1}{2}\int_0^{\ell} \left\{EI(\theta_y'^2 + \theta_z'^2) + kGA\left[(\theta_y - w')^2 + (\theta_z + v')^2\right]\right\}\mathrm{d}s \quad (2)$$

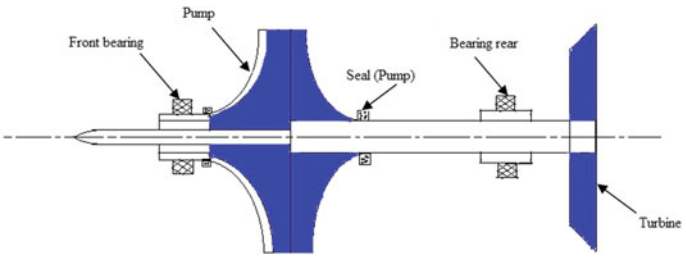

Fig. 1 Turbocharger schematic diagram

The disc kinetic energy can be given as:

$$T_d = \frac{1}{2}m_d\left(\dot{v}^2 + \dot{w}^2\right) + \frac{1}{2}J_d\left(\dot{\theta}_y^2 + \dot{\theta}_z^2\right) + \frac{1}{2}J_p\left[\Omega^2 + \Omega\left(\dot{\theta}_z\theta_y - \dot{\theta}_y\theta_z\right)\right] \quad (3)$$

The mass eccentricity of the disc taken as:

$$W_d = m_d r_d \Omega^2 (w\cos\Omega t + v\sin\Omega t) \quad (4)$$

The translation (v, w) and rotational displacements (θ_y, θ_z) of the shaft element can be approximated by finite element method as:

$$\begin{Bmatrix} v \\ w \end{Bmatrix} = [N_t(s)]\{q\}; \begin{Bmatrix} \theta_y \\ \theta_z \end{Bmatrix} = [N_r(s)]\{q\} \quad (5)$$

where $[N_t(s)]$ and $[N_r(s)]$ are translation and rotational shape functions. By substituting the above expressions into Eqs. (1) and (2) and integrating over the length of the element with Hamilton's principle, the following equation of motion for the shaft and disc units are originated:

$$[M_s]\{\ddot{q}_s\} + \Omega[G_s]\{\dot{q}_s\} + [K_s]\{q_s\} = \{F_s\} \quad (6)$$

$$[M_d]\{\ddot{q}_d\} + \Omega[G_d]\{\dot{q}_d\} = \{F_d\} \quad (7\ \&\ 8)$$

$$[M_s] = \int_0^\ell \rho A[N_t]^T[N_t]\mathrm{d}s + \int_0^\ell \rho I_d[N_r]^T[N_r]\mathrm{d}s; [G_s] = \int_0^\ell \rho I_p[N_r]^T\begin{bmatrix} 0 & 1 \\ -1 & 0 \end{bmatrix}[N_r]\mathrm{d}s$$

$$[K_s] = \int_0^\ell EI[N_r']^T[N_r']\mathrm{d}s + \kappa GA\int_0^\ell \left\{ \begin{matrix} [N_t]^T[N_t] + [N_r]^T[N_r] \\ +2[N_t]^T\begin{bmatrix} 0 & -1 \\ 1 & 0 \end{bmatrix}[N_r] \end{matrix} \right\}\mathrm{d}s \quad (9)$$

By including the effects of damping, the system the equation of motion can be given as [8]

$$[M]\{\ddot{q}\} + [[C] + \Omega[G]]\{\dot{q}\} + [K]\{q\} = \{F\} \quad (10)$$

Here, $F_{py} = m_p e_p \Omega^2 \sin\Omega t - m_p g$ and $F_{pz} = m_p e_p \Omega^2 \cos\Omega t$ are unbalance and gravity forces at the pump, $F_{ty} = m_t e_t \Omega^2 \sin\Omega t - m_t g$ and $F_{tz} = m_t e_t \Omega^2 \cos\Omega t$ are the those at turbine node, while F_{sy} and F_{sz} are component seal forces at the pump along y and z directions, respectively. Here, p-pump, t-turbine, b-bearing, and s-seal forces.

2.2 Seal Force (Nonlinear)

The force expression of the seal model can be given as follows:

$$\begin{Bmatrix} F_{sz} \\ F_{sy} \end{Bmatrix} = -\begin{bmatrix} K_g - m_g\tau_g^2\Omega^2 & \tau_g\Omega D_g \\ -\tau_g\Omega D_g & K_g - m_g\tau_g^2\Omega^2 \end{bmatrix}\begin{Bmatrix} w \\ v \end{Bmatrix} - \begin{bmatrix} D_g & 2\tau_g\Omega m_g \\ -2\tau_g\Omega m_g & D_g \end{bmatrix}\begin{Bmatrix} \dot{w} \\ \dot{v} \end{Bmatrix} - \begin{bmatrix} m_g\ 0 \\ 0\ m_g \end{bmatrix}\begin{Bmatrix} \ddot{w} \\ \ddot{v} \end{Bmatrix} \tag{11}$$

where, K_g, m_g, $D_{g,}$ and τ_g are equivalent stiffness, mass, damping, and the ratios of fluid circumferential velocity, respectively. The all nonlinear functions of the radial displacement of the rotor are follows:

$$K_g = K_0(1 - e^2)^{-n}$$

where,

$$D_g = D_0(1 - e^2)^{-n}(n = 0.5 - 3);\ \tau_g = \tau_0(1 - e)^b(0 < b < 1);\ m_g = \mu_2\mu_3 T_f^2;\ e = \frac{\sqrt{v^2 + w^2}}{c_g}$$

is the relative eccentricity, and it is ratio between the rotor radial displacement to the seal clearance c_g; the coefficients n, b, and τ_0 varies for different kind of seals; in this work, the variables are taken as: $n = 2.5$, $b = 0.5$, and $\tau_0 = 0.49$. The characteristic factors K_0, and D_0 can be calculated from Childs equation [9] as follows: (refer Appendix)

$$K_0 = \mu_3\mu_{0,}\, D_0 = \mu_1\mu_3 T_g \tag{12}$$

where,

$$\mu_0 = \left(\frac{2\sigma^2}{1 + \xi + 2\sigma}\right)E_g(1 - m_0);\ \mu_{1=}\left(\frac{2\sigma^2}{1 + \xi + 2\sigma}\right)\left(\frac{E_g}{\sigma} + \frac{B}{2}\left(\frac{1}{6} + E_g\right)\right);$$
$$\mu_2 = \left(\frac{\sigma}{1 + \xi + 2\sigma}\right)\left(\frac{1}{6} + E_g\right);\ \mu_3 = \left(\frac{\pi R_g\Delta p}{\lambda}\right);\ T_g = \frac{\ell_g}{v_a} \tag{13}$$

Here, $\xi = 0.1$, $n_0 = 0.079$, and $m_0 = -0.25$ and the viscous coefficient of air $\mu = 1.5 \times 10^{-5}$ Pas. The other constants are follows: seal length ℓ_g, seal pressure margin Δp, radius of seal $R_{g,}$ and axial speed of fluid $v_a = \omega R_g$.

2.3 Bearing Forces

The turbopump rotor system is held on ball bearings. The reaction forces at the bearing nodes are in the nature of Hertzian nonlinear radial contact force. The Hertzian contact theory due to nonlinear says that, due to the rolling contact, the force of contact between ball and race is given in terms of Hertzian contact stiffness C_b as:

$$F_{zb} = \sum_{j=1}^{N_b} \left(-C_b(w\cos\theta_j + v\sin\theta_j - r_0)^{3/2} H\right)\cos\theta_j \tag{14}$$

$$F_{yb} = \sum_{j=1}^{N_b} \left(-C_b(w\cos\theta_j + v\sin\theta_j - r_0)^{3/2} H\right)\sin\theta_j \tag{15}$$

where, H can be defined as,

$$H = \begin{cases} 1, \; if \; (w\cos\theta_j + v\sin\theta_j - r_0) > 0 \\ 0, \; if \; (w\cos\theta_j + v\sin\theta_j - r_0) \leq 0 \end{cases} \tag{16}$$

where, $w = w_b + (R - r_0)\,\mathrm{cosq}_j$ and $v = v_b + (R - r_0)\,sinq_j$, θ_j is the angular position of the jth ball, which is having the expressions as,

$$\theta_j = \omega_{\text{cage}} \times t + \frac{2\pi}{N_b}(j-1),\; j = 1, 2, \ldots, N_b \tag{17}$$

3 Numerical Simulation and Discussion

Finite element equations are solved by an interactive method in MATLAB. The physical and mechanical properties of rotor-bearing systems with the dynamic data are listed in Table 1.

The simulated frequencies are found for the system with prompt code as 8.3756, 36.249, 52.887, and 89.683 Hz. Then, the above results are simulated with ANSYS® program and compared with the frequencies from numerical solutions by taking into the effect of rotary inertia (Rayleigh's beam), and listed in Table 2.

The finite element-coupled nonlinear differential equations are solved with Houbolt's implicit time-integration scheme. This method carries last two time steps to calculate the present displacement. To solve the time steps in the equations, central difference method was employed. The second module of numerical simulation was achieved in the program for obtaining frequency response and phase-plane diagrams. Further, convergence study was carried to validate the present numerical codes.

Table 1 Parameters considered for the rotor system

Properties	Values	Properties	Values
Density of shaft material (kg/m^3)	7810	MOI of disc, (kg-mm^2)	41,750 & 168,100($I_{yy} = I_{zz}$)
Young's modulus, E (GPa)	197		83,500 and 336,200 (I_{xx})
Shear modulus, G (GPa)	80	Bearing, r_i (m)	0.031
Radius of shaft (m)	0.012	Bearing, R (m)	0.049
Length of shaft (m)	0.600	Bearing clear. (micr.)	20
Radius of disc (m)	0.15	Bearing stiffness coefficients (N/m)	4×10^7 ($k_{zz} = k_{yy}$)
Thickness of disc (m)	20		1×10^8 ($k_{zz} = k_{yy}$)
No. of balls, N_b	8	Bearing damp. (N/m)	13.34×10^9 (C_b)

Table 2 Frequencies for first three modes from numerical and ANSYS® simulation

Frequency modes		Numerical (Hz)	ANSYS (Hz)	Variation (%)
First	Forward	8.3761	8.4952	1.422
	Backward	8.3756	8.4207	0.538
Second	Forward	36.285	37.322	2.858
	Backward	36.249	37.302	2.905
Third	Forward	53.217	54.105	1.669
	Backward	52.882	53.647	1.447

The summary of results for different set of elements from convergence study is listed in Table 3. The investigation reveals that the frequencies are converges.

Figure 2 shows the time histories of pump and turbine nodes for z displacements (left) and y displacements (right) for the angular velocity of, $\Omega = 1000$ rpm for the time period of 10 s. The displacement curves shows that the amplitude is getting reduced due to the nonlinear effects from the seals at both the bearing housings.

Remarks 1 Boundary conditions follow with the initial assumptions of the system with the disc unbalance, $e = 0.001$ m, and gravity as well as the viscoelastic force components are treated as external forces. The reaction forces at the bearing nodes are in the nature of Hertzian nonlinear radial contact force. Based on the parameters given in Table 1, the dynamic response of the rotor systems are plotted in Figs. 2 and 3.

Table 3 Convergence study for numerical simulation

Freq.	Whirl modes (Hz)	Number of elements			Freq.	Whirl modes (Hz)	Number of elements		
		4	8	12			4	8	12
1st	Forward	8.3761	8.3752	8.3748	2nd	Backward	36.249	36.242	36.238
	Backward	8.3756	8.3748	8.3740	3rd	Forward	53.217	53.211	53.206
2nd	Forward	36.285	36.274	36.269		Backward	52.882	52.874	52.865

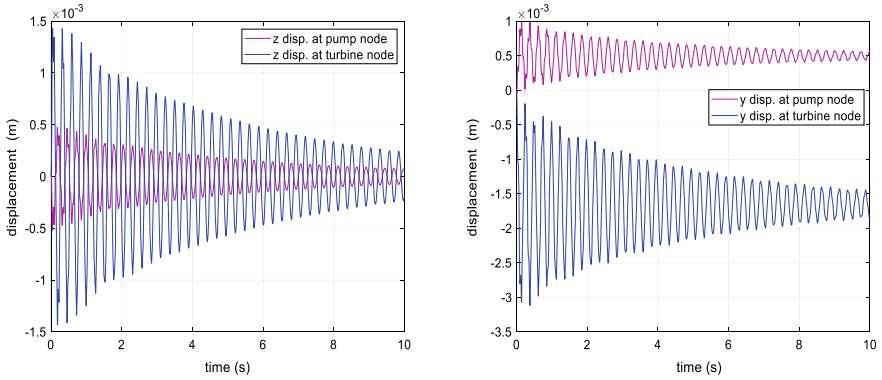

Fig. 2 Time histories of pump and turbine nodes for the angular velocity of, $\Omega = 1000$ rpm

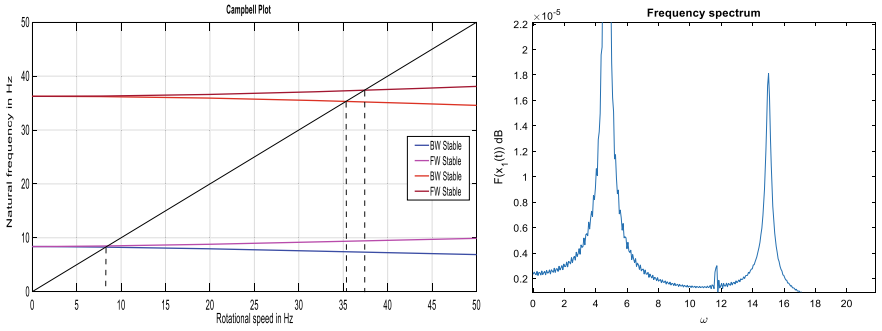

Fig. 3 Campbell plot for $\Omega = 3000$ rpm and frequency spectrum of rotor at $\Omega = 1000$ rpm

4 Conclusions

Simulated vibrations of automotive turbocharger rotor supported in bearings were studied and presented with nonlinear hydrodynamic seal forces. The system modelled with Timoshenko beam theory and analysis was carried by using finite element method. At the bearing supports which mounted on the base is experiencing the excitation and the same is transferred to the rotor. The systems include the force due to imbalance, gyroscopic, bearing reactions and the effect of gravity also into account for the specific operational speed level in the dynamic study and have been presented. The results are shown in Figs. 2, 3 and 4. The simulated numerical solutions are compared with the frequencies with ANSYS® program which are listed in Table 2. Furthermore, convergence study was carried to validate the present numerical codes for three set of elements and listed in Table 3. In theoretical analysis, for the large whirling amplitudes can be accounted and studied through the impact of external/nonlinear seal force analysis in the same approach. The system becomes stable (periodic) after 15,000 rpm, and from the results, it is obvious that, due to the

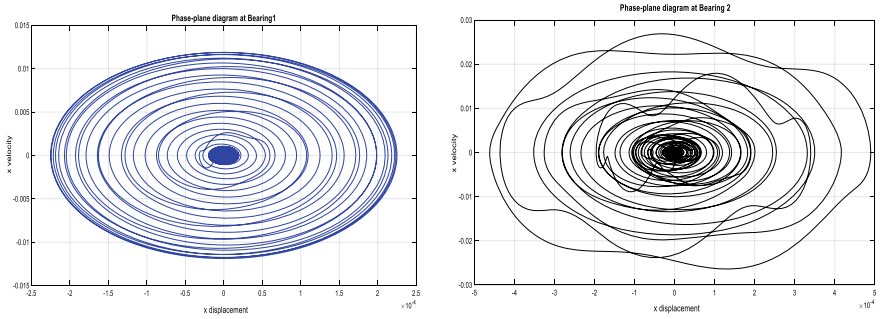

Fig. 4 Phase-plane diagrams of bearing1 (left) and 2 (right) with $\Omega = 1000$ rpm

nonlinear dynamic forces of turbopump rotor system, the sub-synchronous motion is observed.

Appendix

$$\lambda = n_0 (R_a)^{m0} \left[1 + \left(\frac{R_v}{R_a} \right)^2 \right]^{(1+m_0)/2} ; \sigma = \frac{\lambda \ell_g}{c_g}; E_g = \frac{1+\xi}{2(1+\xi+2\sigma)}; B = 2 - \frac{(R_v/R_a)^2 - m_0}{(R_v/R_a)^2 + 1};$$

$$R_v = \frac{R_g \omega c_g}{\mu}; R_a = \frac{2 v_a c_g}{\mu}$$

References

1. Bai C, Xu Q, Wang J (2011) Effects of flexible support stiffness on the nonlinear dynamic characteristics and stability of a turbopump rotor system. Nonlinear Dyn 64:237–252. https://doi.org/10.1007/s11071-010-9858-4
2. Son M, Koo J, Cho WK, Lee ES (2012) Conceptual design for a kerosene fuel-rich gas-generator of a turbopump-fed liquid rocket engine. J Therm Sci 21:428–434. https://doi.org/10.1007/s11630-012-0564-z
3. Hu L, Hu N, Fan B, Gu F (2012) Application of novelty detection methods to health monitoring and typical fault diagnosis of a turbopump. J Phys Conf Ser 364. https://doi.org/10.1088/1742-6596/364/1/012128
4. Hong SS, Kim DJ, Kim JS et al (2013) Study on inducer and impeller of a centrifugal pump for a rocket engine turbopump. Proc Inst Mech Eng Part C J Mech Eng Sci 227:311–319. https://doi.org/10.1177/0954406212449939
5. Wang JF, Sun K (2012) The calculation of the rotor critical speed of turbopump. Adv Mater Res 529:220–223. https://doi.org/10.4028/www.scientific.net/amr.529.220
6. Smolík L, Hajžman M, Byrtus M (2017) Investigation of bearing clearance effects in dynamics of turbochargers. Int J Mech Sci 127:62–72. https://doi.org/10.1016/j.ijmecsci.2016.07.013

7. Novotný P, Škara P, Hliník J (2018) The effective computational model of the hydrodynamics journal floating ring bearing for simulations of long transient regimes of turbocharger rotor dynamics. Int J Mech Sci 148:611–619. https://doi.org/10.1016/j.ijmecsci.2018.09.025
8. Nelson HD (2010) A finite rotating shaft element using timoshenko beam theory. J Mech Des 102:793. https://doi.org/10.1115/1.3254824
9. Childs DW (2009) Dynamic analysis of turbulent annular seals based on hirs' lubrication equation. J Lubr Technol 105:429. https://doi.org/10.1115/1.3254633